Figures 1 and 2 show typical potential-dependent sequences of SER spectra obtained for a C_{60} film (two to three monolayers thick) in the 240–840-cm^{-1} and 1080–1620-cm^{-1} frequency regions, respectively, every 10 s during a cyclic voltammogram at 10 mV s^{-1} between 0 and −1.2 V vs $Fc^{+/0}$. (The spectra are limited to 500–600-cm^{-1} segments due to the spatial characteristics of the CCD detector at 647 nm. No significant spectral features were observed from 800 to 1050 cm^{-1}.) The potentials labeled alongside each spectrum are the average values during the data acquistion; the spectra are stacked so that the upward sequence refers to increasing time.

At potentials positive of ca. −0.9 V, the SER spectral features are uniformly quite similar to the normal Raman bands reported for solid bulk-phase C_{60};[1] the frequencies typically match within 5–10 cm^{-1}, and the relative intensities are comparable. A summary of these SER bands, along with the corresponding bulk-phase Raman frequencies, is given in Table I. All 10 Raman active bands anticipated from the bulk-phase selection rules (having A_g or H_g symmetry)[1] are apparently also observed in the SER spectra. Three additional weaker bands are observed, with frequencies that match closely those reported in the bulk-phase infrared spectrum. The one remaining infrared-active band (at 1428 cm^{-1}) is accidentally degenerate with a Raman-active feature. Consequently, then, the SERS selection rules allow the normally exclusively infrared active as well as Raman-active modes of C_{60} to be observed. This symmetry lowering would appear to occur in the absence of C_{60}-surface coordination; the appearance of such Raman-forbidden bands probably reflects the influence of the surface electric-field gradient.[12] The present results differ somewhat from a recent report of SERS for C_{60} on gold in aqueous media, for which a number of additional bands, attributed to distorted C_{60} species, were observed.[2]

The present SERS features are virtually independent of potential between 1.0 and ca. −0.7 V and of the film thickness (from ca. 2 to 20 monolayers). Significant spectral changes, however, occur at potentials between −0.9 and −1.1 V during the forward (negative-going) sweep, which are reversed at ca. −0.6 V during the return sweep (Figures 1 and 2). These potentials correspond precisely to the appearance of the anodic and cathodic waves associated with the formation and reoxidation of C_{60}^- (cf. ref 7).

Several significant elements of these redox-induced spectral changes are evident, as can be seen from Figures 1 and 2 and Table I. First, some of the Raman active bands undergo significant (ca. 5–20 cm^{-1}) frequency downshifts upon formation of C_{60}^- from C_{60}, most prominently for the C_{60} A_g mode at 1460 cm^{-1}, which downshifts by almost 20 cm^{-1}. A comparable frequency downshift for this Raman band has been seen upon doping C_{60} with alkali metals so as to yield conducting films.[13] These effects are indicative of the weakening of C–C bonds caused by the added antibonding electron. Additionally, several bands having H_g symmetry become more intense and broader upon C_{60}^- formation; moreover, two bands (at ca. 710 and 770 cm^{-1}) yield doublets (Figure 1). These changes may well reflect a loss of the usual 5-fold degeneracy of the H_g symmetry bands, arising from anticipated Jahn–Teller distortions in the monoanion.[4b] Sweeping the potential to values negative of −1.4 V, corresponding to C_{60}^{2-} formation, yielded further frequency downshifts of the major Raman features. The bands, however, become markedly weaker and broader. Nonetheless, spectra corresponding to C_{60}^- and C_{60} reappear upon returning the potential to appropriately less negative potentials.

Acknowledgment. Xiaoping Gao provided expert guidance in spectral interpretation. The C_{60} sample was prepared by Joe Roth and Lance Safford. This work is supported by the National Science Foundation and the Office of Naval Research.

(12) (a) Moskovits, M.; DiLella, D. P.; Maynard, K. J. *Langmuir* **1988**, *4*, 67. (b) Moskovits, M. *Rev. Mod. Phys.* **1985**, *57*, 783.
(13) Haddon, R. C.; Hebard, A. F.; Rosseinsky, M. J.; Murphy, D. W.; Duclos, S. J.; Lyons, K. B.; Miller, B.; Rosamilia, J. M.; Fleming, R. M.; Korton, A. R.; Glarum, S. H.; Makhija, A. V.; Muller, A. J.; Erick, R. H.; Zahwak, S. M.; Tycko, R.; Dabbagh, G.; Thiel, F. A. *Nature* **1991**, *350*, 320.

Antibody-Catalyzed Hydrolysis of Phosphate Monoesters

Thomas S. Scanlan, James R. Prudent, and Peter G. Schultz*

Department of Chemistry, University of California Berkeley, California 94720

Received July 18, 1991

Phosphoryl transfer reactions involving tyrosine, serine, or threonine residues play an important biological role in many regulatory and signal transduction processes. Catalysts which selectively phosphorylate or dephosphorylate a given peptide sequence would provide important tools for investigating these systems.[1] One approach to generating catalysts that recognize a specific phosphorylation site takes advantage of the specificity of the antibody molecule.[2] As a first step toward the development of a family of catalytic antibodies for selective phosphoryl transfer reactions, we report the generation of antibodies that catalyze the hydrolysis of an aryl phosphate monoester.

The hapten α-hydroxyphosphonate **1** was synthesized in six steps from α-bromotoluic acid[3] and coupled to keyhole limpet hemocyanin (KLH) via a diazo-linkage reaction to generate an immunogenic conjugate.[4] Balb/C mice were immunized with the

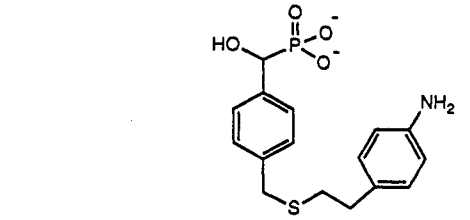

1

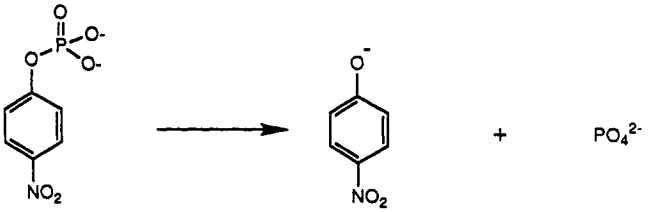

2 (p-NPP)

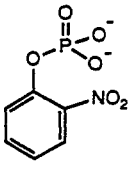

3

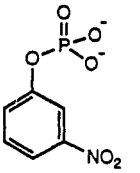

4

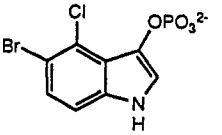

5

protein–hapten conjugate, and 20 hapten-specific hybridoma cell lines were generated using standard hybridoma technology.[5] Monoclonal antibodies from these hybridomas were purified to homogeneity (SDS–polyacrylamide gel electrophoresis) from ascites fluid by protein A affinity chromatography.[6] The antibodies were then assayed spectrophotometrically for their ability

* Author to whom correspondence should be addressed.

(1) For model systems, see: (a) Chin, J.; Banaszczyk, M. *J. Am. Chem. Soc.* **1989**, *111*, 4103. (b) Breslow, R.; Singh, S. *Bioorg. Chem.* **1988**, *16*, 408.
(2) (a) Lerner, R. A.; Benkovic, S. J.; Schultz, P. G. *Science* **1991**, *252*, 659. (b) Schultz, P. G.; Lerner, R. A.; Benkovic, S. J. *Chem. Eng. News* **1990**, *68*, 26.
(3) α-Bromotoluic acid and *p*-nitrophenethyl mercaptan were coupled to form the corresponding thioester–carboxylic acid. Acid chloride formation ($SOCl_2$) followed by an Arbuzof reaction (triethyl phosphite) and carbonyl reduction (DIBAL-H) provided the protected 2-hydroxy aryl phosphonate. Reduction of the nitro group ($SnCl_2$) and phosphonate ester hydrolysis (TMSBr) afforded racemic hapten **1**.
(4) Erlanger, B. *Methods Enzymol.* **1980**, *70*, 85.
(5) Kohler, G.; Milstein, C. *Nature (London)* **1975**, *256*, 495.
(6) Kronvall, G.; Grey, H.; Williams, R. *J. Immunol.* **1972**, *105*, 1116.

0002-7863/91/1513-9397$02.50/0

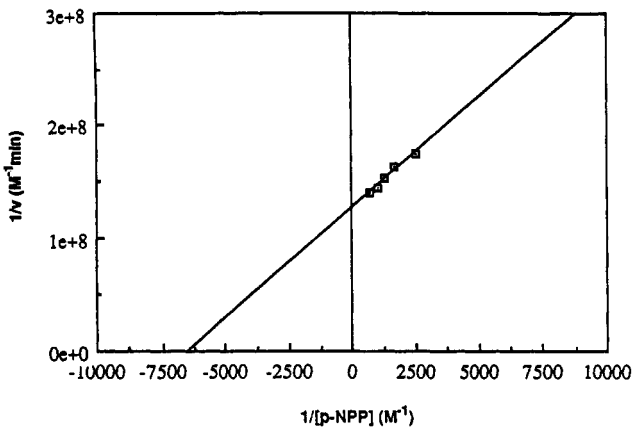

Figure 1. Lineweaver-Burk plot of 38E1-catalyzed hydrolysis of *p*-NPP: [38E1] = 6.7 μM in 50 mM CHES, 25 mM NaCl, pH 9.0; [*p*-NPP] = 1.5, 1.0, 0.8, 0.6, 0.4 mM. Velocity measurements were performed in triplicate at each substrate concentration, monitoring the increasing absorbance at 400 nm corresponding to the formation of *p*-nitrophenolate ion.

to catalyze the hydrolysis of *p*-nitrophenyl phosphate **2** (*p*-NPP). Five of the 20 antibodies were found to catalyze the hydrolysis of the phosphate monoester at a significant rate above the uncatalyzed background reaction. One of these antibodies (38E1) was characterized in more detail.

The *p*-NPP hydrolysis reaction catalyzed by 38E1 displayed a pH optimum at alkaline pH; consequently, all kinetic parameters were measured in the presence of 6.7 μM antibody 38E1 in 50 mM CHES [2-(*N*-cyclohexylamino)ethanesulfonic acid], 25 mM NaCl at pH 9.0.[7] Under these conditions, 38E1 catalyzed the hydrolysis of *p*-NPP in a manner consistent with Michaelis-Menten kinetics.[8] A Lineweaver-Burk plot (Figure 1) of the steady-state data afforded a k_{cat} of 0.0012 min^{-1} and a K_M of 155 μM. The observed first-order rate constant for the uncatalyzed hydrolysis of *p*-NPP in the same buffer system was determined to be 1.5×10^{-7} min^{-1}. Greater than 11 turnovers per antibody molecule were measured with no apparent change in V_{max}, demonstrating that the antibody functions catalytically.

The Fab fragment of 38E1, generated by partial papain digestion,[9] retained the catalytic activity of the intact IgG, supporting the concept that catalysis occurs in the antibody combining site. The antibody 38E1 also retained activity in the presence of the metal chelator EDTA, which abolishes the catalytic activity of the metal-dependent phosphatases.[10] Moreover, several ester- and carbonate-cleaving catalytic antibodies have been generated in our laboratory from haptens containing nitrophenyl phosphonate substructures, and none of these antibodies were found to catalyze the hydrolysis of *p*-NPP.[11]

The antibody-catalyzed reaction was competitively inhibited by hapten **1**. A Dixon analysis[12] with hapten **1** afforded a K_i of 34 μM. The V_{max} value of 1.0×10^{-8} min^{-1} derived from the Dixon plot was in good agreement with the V_{max} value obtained from the Lineweaver-Burk analysis. The substrate specificity of antibody 38E1 was also examined. Phosphate monoesters **3-5** were found to be poor substrates for antibody 38E1, with hydrolytic rates barely detectable above the uncatalyzed reaction.[13] This high level of specificity, favoring the para-substituted phenyl phosphate, is consistent with an antibody-catalyzed reaction and most likely derives from the para-substituted aryl ring of hapten **1**. In contrast, alkaline phosphatases from a wide range of sources exhibit low substrate specificity, hydrolyzing positional isomers of aryl phosphates with similar rates.[14]

Mechanistic aspects of this antibody-catalyzed reaction are currently being explored, including both electrostatic catalysis and the notion that hapten **1**, like the less stable vanadate esters, mimics a species involved in attack of water on the phosphate monoester. In fact, it has been reported that 2-hydroxy carboxylic acids and tartrates, which are structural analogues of hapten **1**, act as inhibitors of phosphatase enzymes.[15] Consequently, a more detailed understanding of the structural features of hapten **1** leading to antibody catalysis could provide a new class of selective phosphoryl-transferase enzyme inhibitors.

Acknowledgment. We acknowledge the helpful assistance of James Stephens and Tam Dinh and financial support by the Office of Naval Research (Grant No. N00014-87-K-0256). T.S.S. acknowledges the Damon Runyon-Walter Winchell Cancer Research Fund (DRG-1016) for support through a postdoctoral fellowship, and P.G.S. is an NSF Alan T. Waterman awardee.

(7) All kinetic assays were performed on a Kontron Uvikon 860 spectrophotometer. Reaction volumes of 1.2 mL were used, and time-point measurements were recorded at 400 nm (λ_{max} for *p*-NPP, $\epsilon = 17\,000$ M^{-1} cm^{-1}) in 1-mL cuvettes. Typically, a 50× concentrated substrate stock solution in water was diluted into a solution of the antibody sample in 50 mM CHES, 25 mM NaCl, pH 9.0 assay buffer. The reactions were incubated at 30 °C, and time points were recorded over a 30-h reaction period. Under these conditions, the hydrolysis reaction proceeded to <5% completion.

(8) Fersht, A. *Enzyme Structure and Mechanism*, 2nd ed.; W. H. Freeman and Company: New York, 1985; Chapter 3, pp 98-118.

(9) Papain (200 μg, Sigma) was added to a solution of antibody 38E1 (20 mg) in 100 mM $NaHPO_4$, 4 mM EDTA, 1 mM DTT at pH 7.2. The reaction mixture was incubated for 4 h at 37 °C and passed down a 1.5 × 100 cm G-50 sizing column eluting with 10 mM $NaHPO_4$, 150 mM NaCl, pH 7.2, to remove the papain. The eluted protein was then passed down a 1 × 4 cm sepharose-coupled protein A column, and the void volume material was collected. The purified Fab was then concentrated by vacuum dialysis. Fab prepared by this procedure was found to be >95% pure as judged by SDS-polyacrylamide gel electrophoresis with Coomassie Blue staining.

(10) Ackermann, B. P.; Ahlers, J. *Biochem. J.* **1976**, *153*, 151.

(11) Jacobs, J.; Pollack, S.; Schultz, P. G., unpublished results.

(12) Dixon, M. *Biochem. J.* **1953**, *55*, 170.

(13) Substrates **5** (5-bromo-4-chloro-3-indolyl phosphate) is commercially available (Sigma). Substrates **3** and **4** were synthesized by the method of Kirby and Varvoglis: Kirby, A. J.; Varvoglis, A. G. *J. Am. Chem. Soc.* **1967**, *89*, 415.

(14) (a) Fernley, H. N.; Walker, P. G. *Nature (London)* **1966**, *212*, 1435. (b) Lynn, K. R.; Clevette-Radford, N. A.; Chaqui, C. A. *Bioorg. Chem.* **1981**, *10*, 90. (c) Garen, A.; Levinthal, C. *Biochim. Biophys. Acta* **1960**, *38*, 470.

(15) Kilsheimer, G. S.; Axelrod, B. *J. Biol. Chem.* **1957**, *227*, 879.

Engineering Protein Specificity: Gene Manipulation with Semisynthetic Nucleases

Dehua Pei and Peter G. Schultz*

Department of Chemistry, University of California Berkeley, California 94720

Received July 22, 1991

During the past decade, site-directed mutagenesis and chemical modification have been extensively used in attempts to engineer proteins with novel functions or altered specificities. For example, mutagenesis has been used to alter the specificities of aspartate aminotransferase, a dehydrogenase, and 434 repressor, and semisynthesis has been used to generate a redox-active flavopapain.[1] By using a combination of *both* chemical and genetic approaches, we were able to convert a relatively nonspecific phosphodiesterase, staphylococcal nuclease, into a molecule capable of sequence-specifically hydrolyzing RNA, single-stranded DNA, and duplex DNA.[2,3] Adducts of staphylococcal nuclease with either oligo-

* Author to whom correspondence should be addressed.

(1) (a) Cronin, C. N.; Malcolm, B. A.; Kirsch, J. F. *J. Am. Chem. Soc.* **1987**, *109*, 2222-2223. (b) Scrutton, N. S.; Berry, A.; Perham, R. N. *Nature* **1990**, *343*, 38-43. (c) Wharton, R. P.; Ptashne, M. *Nature* **1985**, *316*, 601-605. (d) Kaiser, E. T.; Lawrence, D. S. *Science* **1984**, *226*, 505-511.

(2) (a) Corey, D. R.; Pei, D.; Schultz, P. G. *J. Am. Chem. Soc.* **1989**, *111*, 8523-8525. (b) Pei, D.; Schultz, P. G. *J. Am. Chem. Soc.* **1990**, *112*, 4579-4580. (c) Corey, D. R.; Schultz, P. G. *Science* **1987**, *238*, 1401-1403. (d) Corey, D. R.; Pei, D.; Schultz, P. G. *Biochemistry* **1989**, *28*, 8277-8286. (e) Zuckermann, R. N.; Schultz, P. G. *Proc. Natl. Acad. Sci. U.S.A.* **1989**, *86*, 1766-1770.

(3) Pei, D.; Corey, D. R.; Schultz, P. G. *Proc. Natl. Acad. Sci. U.S.A.* **1990**, 9858-9862.

0002-7863/91/1513-9398$02.50/0